
Article:
Scalisi, J., Oxley, W., Ruderman, M.S. orcid.org/0000-0003-2324-8466 et al. (1 more author) (2021) Propagation of torsional Alfvén pulses in zero-beta flux tubes. The Astrophysical Journal, 911 (1). 39. ISSN 0004-637X

https://doi.org/10.3847/1538-4357/abe8db

Draft version April 22, 2021
Typeset using LaTeX default style in AASTeX63

Propagation of Torsional Alfvén Pulses in Zero-beta Flux Tubes

Joseph Scalisi,[1] William Oxley,[1] Michael S. Ruderman,[1,2] and Robertus Erdélyi[1,3,4]

[1] *Solar Physics and Space Plasma Research Centre, School of Mathematics and Statistics, University of Sheffield, Hicks Building, Hounsfield Road Sheffield, S3 7RH, UK*

[2] *Space Research Institute (IKI), Russian Academy of Sciences, Moscow, Russia*

[3] *Department of Astronomy, Eötvös Loránd University, 1/A Pázmány Péter sétány, H-1117, Budapest, Hungary*

[4] *Gyula Bay Zoltán Solar Observatory (GSO), Hungarian Solar Physics Foundation (HSPF), Petőfi tér 3., Gyula, H-5700, Hungary*

ABSTRACT

In this study, we investigate analytically the generation of mass flux due to a torsional Alfvén pulse. We derive that the presence of torsional Alfvén waves, which have been observed in e.g. photospheric magnetic bright points (MBPs), can result in vertical plasma motions. The formation of this mass flux may even be a viable contribution to the generation of chromospheric mass transport, playing potential roles in the form of localised lower solar atmospheric jets. This relationship is studied using a flux tube model, with the waves introduced at the lower boundary of the tube as a magnetic shear perturbation. Due to the nature of MBPs we simplify the model by using the zero-beta approximation for the plasma inside the tube. The analytical results are demonstrated by an example of the type of Alfvén wave perturbation that one might expect to observe, and comparison is made with properties of spicules known from observations. We find that field-aligned plasma flux is formed non-linearly as a result of the Lorentz force generated by the perturbations, and could be consistent with jet formation, although the current model is not intended to determine the entire evolution of a jet. Critical discussion of the model follows, including suggestions for improvements and for high-resolution proposed observations in order to constrain the driving magnetic and velocity shear.

1. INTRODUCTION

In recent decades, technological developments have enabled direct observation of increasingly refined details of solar activity. Ground-based telescopes such as the Swedish Solar Telescope (SST) have allowed observations of smallest-scale features, including magnetic bright points (MBPs) (Jess et al. 2009; Liu et al. 2018), and magnetic swirls (Liu et al. 2019b). Meanwhile space-based platforms including the Solar and Heliospheric Observatory (SOHO) and Solar Dynamics Observatory (SDO) allow for advanced spectral imaging, enabling us to view the solar atmosphere at certain wavelengths not visible from Earth, including features such as spicules, and the larger and less common macrospicules (Withbroe et al. 1976; Kiss et al. 2017) which appear in extreme ultraviolet (EUV).

Solar jets are a category of lower solar atmospheric phenomena of great interest (Beckers 1968, 1972; Sterling 2000; Tsiropoula et al. 2012). Understanding different types of jet, particularly spicules and macrospicules, is a major goal for solar research given their ubiquity and therefore their role in the mass, momentum, and energy transport of the lower solar atmosphere. In particular, since they are able to transfer vast amounts of mass and momentum higher into the atmosphere (Athay & Holzer 1982; De Pontieu et al. 2004), jets are a viable source for the material that makes up the solar wind. They are also thought to act as waveguides and allow magnetohydrodynamic (MHD) waves to propagate towards the outer solar atmosphere (De Pontieu et al. 2007; Zaqarashvili & Erdélyi 2009; Dover et al. 2020), carrying energy and potentially contributing to the extreme temperature of the corona. Aside from this, jets are widely studied because they are observed constantly throughout the solar atmosphere, and in many different variations (Raouafi et al. 2016; Bennett & Erdélyi 2015). The process by which these jets form is not certain. A wide range of mechanisms are proposed including, for example, granular buffeting (Roberts 1979), MHD waves and/or shocks (Hollweg 1982; Dover et al. 2020), global solar (p-mode) oscillation (Suematsu 1980; De Pontieu et al. 2004), magnetic

Corresponding author: Róbert Erdélyi
robertus@sheffield.ac.uk

reconnection (Samanta et al. 2019), Lorentz force (Shibata & Uchida 1986), and ambipolar diffusion (Martínez-Sykora et al. 2017).

Spicules were first observed in 1877 by Secchi (Secchi 1877), but despite their long history of study (Beckers 1968; Sterling 2000; Tsiropoula et al. 2012), their nature is still not fully understood. They are relatively small (reaching around 7–13Mm in height), thin (with widths around 0.3–1.5Mm), and short-lived jets (lasting under 10 minutes) made up of fast-moving plasma, as reviewed e.g by Sterling (2000). It has been suggested that there are two main types of spicule, with a distinction between those which rise and then fall (i.e. the "traditional" Secchi-type) and those which appear to fade away in hot coronal channels referred to as rapid blue excursions (RBEs) (Rouppe van der Voort et al. 2009; Kuridze et al. 2015) or also known as Type II spicules, see e.g. De Pontieu et al. (2007). Type II spicules are thought to be faster and smaller than the "Secchi-type" chromospheric H-alpha spicules, with heights between 1–5Mm and with diameters of 120-700km (De Pontieu et al. 2007; Sterling et al. 2010).

MBPs and spicules are close to the lower limit of the resolution we can currently observe even with the SST, Big Bear Solar Observatory (BBSO), or New Vaccuum Solar Telescope (NVST). Appearing in the chromosphere in vast numbers, spicules create the appearance of 'grass', and are visible at the solar limb; although we can clearly see their vertical extents, it is difficult to observe their internal structures and the process of their formation. MPBs are examples of intense magnetic flux tubes and occur frequently at supergranule boundaries (Keys et al. 2013; Dunn & Zirker 1973), the same region we observe high concentrations of spicules (Tsiropoula et al. 2012). Therefore assuming a connection between MBPs and spicules is a reasonable conjecture and working hypothesis. Further study of this connection between MBPs and spicules would be highly useful, and perhaps the Daniel K. Inouye Solar Telescope (DKIST) will enable a breakthrough on the observational side of this; see DKIST Science Use Cases (https://nso.edu/telescopes/dkist/csp) e.g. SUC178.

Over the years there have been a number of theoretically proposed mechanisms by which jets and spicules may form, as we already outlined above briefly. The non-linear MHD system is difficult to solve even numerically, let alone analytically, but access to greater computing power has lead to advanced MHD simulations (Matsumoto & Shibata 2010; Martínez-Sykora et al. 2017; González-Avilés et al. 2018; Magyar et al. 2021). In spite of the theoretical challenges, some authors have made attempts to model jets using analytical approaches (Goodman 2012). Analytical modelling can be useful as a first approximation for the behaviour of the system and gives an important alternative perspective to observations and simulations. In this paper, we will also embark on an analytical approach.

Goodman (2012) attempted to model the acceleration of spicules by specifying a current which would generate an associated Lorentz force, and used the momentum equation to obtain the plasma velocity. Unfortunately, the method implemented by Goodman (2012) may not be applicable, as the full MHD system (e.g. including the induction equation) is not considered properly in that paper and the equations are not satisfied. Hence the specified current and results are not valid for spicule formation. The concept itself is, however, reasonable and should be explored further with mathematical rigour. Consequently, we re-evaluate the approach of Goodman (2012) as part of the inspiration for the study presented here.

Another analytical study of note is Hollweg (1971), in which a perturbation method is utilised to investigate the second-order non-linear effects of Alfvén waves propagating in the direction of a background magnetic field. The study concentrates on density perturbations and is not explicitly related to jets or spicules, but we believe the method could be adapted to this purpose. In particular, an analytical method was used to study the non-linear effects of Alfvén waves by considering multiple perturbation scales. We have employed similar techniques in our work, with applications such as different equilibrium conditions and perturbation structure, and a 3D coordinate system rather than only transverse and longitudinal components. The same author provides an example of a numerical approach to the study of spicule formation in Hollweg (1982) with a focus on the role of Alfvén waves which, when non-linear processes are taken into account, may result in rebound shocks.

Building on the preceding work of Hollweg et al. (1982), the study of Hollweg (1982) presents the concept that spicules may form when the chromosphere is thrust upwards by these rebound shocks. In our analytical work, however, we find and argue that these shocks may not be necessary for spicule formation. Instead, weakly non-linear Alfvén waves may drive secondary perturbations *without* the development of shocks, directly triggering plasma movement which then may be identified with spicules. This also highlights the importance of using various approaches to study these features, as it is likely that multiple processes contribute to the excitation of jets.

One suggestion for the spicule mechanism proposed by Haerendel (1992) was that momentum may be transferred to the plasma by the damping of upwards-moving Alfvén waves due to ion-neutral collisions. This was explored further

via numerical simulations by e.g. James & Erdélyi (2002); James et al. (2003), who found that spicules could not be convincingly recreated with the model, but also stated that the mechanism may still play a part in spicule formation due to the temperatures achieved in the simulations. A later study by Martínez-Sykora et al. (2017) found that ion-neutral interactions allowed magnetic tension to be transported upwards and may be important for spicule formation. Therefore, one may conclude that Alfvén waves may indeed be important in the formation of spicules, though the micro-physics is yet to be determined.

The evolution of an Alfvén pulse was studied in Verwichte et al. (1999), using both analytical and numerical methods. This study utilised a perturbation method and assumed a homogeneous cold plasma, i.e. zero-beta. Although the study was not specific to solar jets, it was found that density perturbations and field-aligned plasma flows were possible as a result of this type of Alfvén wave. Consequently, a similar concept could be applicable to spicules and so we incorporate some aspects from this into our model.

Magnetically-driven jets have also been studied in the context of astrophysical phenomena of various scales (Shibata & Uchida 1985; Innes et al. 1997; Smith 2012), in addition to solar jets. Building on their earlier work relating to other astrophysical jets, Shibata & Uchida (1986) suggested a mechanism for solar jets involving a packet of magnetic twist driving mass along a flux tube, which they studied numerically. The idea of spicules driven by the Lorentz force (and the role of Alfvén waves in this process) requires further research and inspired us to construct our own model. We use a perturbation method and consider magnetic shear in the form of a torsional Alfvén wave pulse, justified by a recent observational finding that also shows strong links with magnetic flux concentrations (Liu et al. 2019a,b), which provides the necessary Lorentz force.

The model presented in this study, for the sake of simplicity, uses a straight flux tube configuration and is an idealised description of the real solar atmosphere. Various additional assumptions are made for further simplicity, such as taking the plasma-beta to be zero, using an axially symmetric cylinder, and assuming no stratification. Nonetheless, we can still apply the model as a starting point for the analytical study. In Section 2, a more detailed physical explanation of the model is given. The model itself is then further defined and used to derive some useful and applicable properties in Section 3, along with a specific example which is employed to investigate the potential application of the model to observed solar phenomena. This is followed by a critical discussion of the results in Section 4 along with theoretical comparison with known properties of jets.

2. PHYSICAL CONSIDERATIONS

Shear flows, or equivalently a shear in the magnetic field due to the highly frozen-in property of the lower solar atmospheric plasma, may be capable of exciting vertical plasma motion, i.e. mass and momentum transport, due to the rise of the local Lorentz force. In particular, we focus on the role of torsional Alfvén waves, which have been observed in connection to MBPs (Jess et al. 2009) and swirls (Liu et al. 2019b); we are particularly interested in MBPs as an example to demonstrate our point. It is thought that MBPs appear bright because through them we can observe deeper into the solar atmosphere (Berger et al. 2007; Sánchez Almeida et al. 2010), almost like looking through a tube. This, along with the cylindrical shape of the jets themselves, will motivate our choice of model. Our aim is to investigate the non-linear behaviour of a torsional Alfvén pulse to find a viable mechanism by which spicules may be formed, such that i) their ubiquity is accounted for and ii) including their connection to localised magnetic waveguide features, e.g. magnetic bright points.

Consider a straight cylindrical magnetic flux tube (see Figure 1) located in the lower solar atmosphere, anchored in a magnetic bright point in the photosphere and surrounded by the quiet Sun. Observations suggest MBPs have diameters up to around 0.5Mm (Berger et al. 1995; Liu et al. 2018), and a reasonable estimate for the tube radius is $R_0 = 0.15$Mm. Magnetic shear is introduced via a torsional Alfvén wave perturbation confined within the flux tube, originating at the 'base' of the tube ($z = 0$) which we consider to be roughly at the height of the photosphere-chromosphere interface. The perturbation then propagates upwards as a pulse, travelling along the tube towards the upper chromosphere. Flux tube models, as building blocks of the solar atmosphere, are a versatile tool for solar applications (Mathioudakis et al. 2013; Ryutova 2015) and a tube with magnetic shear is a good and reasonable fit for the physical configuration we are interested in.

Although we are using a simplified model, the problem is complex in the general non-linear case, even when some higher order terms are neglected. One way to approach the problem is to consider the zero plasma-beta case, an approximation that is relevant in regions of dominant magnetic field strength when compared to the plasma pressure. Since MBPs are known to have considerably lower kinetic pressure than their surrounding plasma and have field

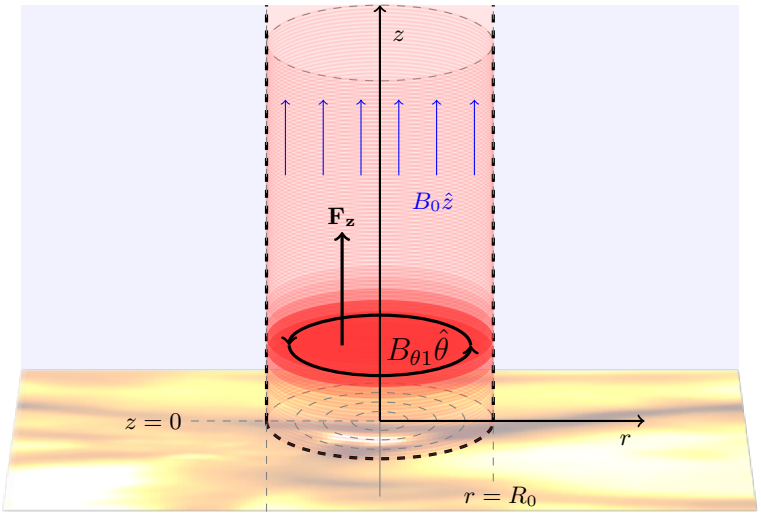

Figure 1. The flux tube in the region $r < R_0$ and $z > 0$, with the torsional perturbation shown in darker red. The perturbation is an Alfvén pulse originating at $z = 0$ and propagating vertically up the tube. The vertical force $F_z = (\mathbf{j} \times \mathbf{B})_z$ is the z-component of the Lorentz force. The vertical magnetic field $B_0\hat{z}$, shown by the blue arrows, is constant inside the tube. The bottom panel of the image is adopted from Daniel K. Inouye Solar Telescope and is used for illustrative purposes only; credit due to NSO/NSF/AURA.

strength on the order of a kilogauss (Keys et al. 2013), this approximation is appropriate for our purpose of modelling the lower atmospheric roots of MBPs. In the general case, we also assume total pressure is balanced at the boundary of the tube. Applying the zero-beta approximation inside the tube will allow us to consider this region independently and ignore the plasma pressure gradient, therefore enabling us to isolate the vertical component of the Lorentz force that directly results from the shear perturbation.

3. MODEL

Using the regular perturbation method (Hinch 1991) we model the effect of a localised magnetic field disturbance in the form of magnetic shear, and focus on the resulting Lorentz force. The model could be applicable to the aforementioned magnetic bright points and swirls, which have the potential to generate magnetic wave fields comparable to the perturbation we consider. It should be emphasised that we use standard methods and the well-known ideal MHD equations, and as such the model discussed here shares properties with and builds on the methods of some works mentioned in Section 1 such as Hollweg (1971). However, our application is different and we specify the model for our purposes.

Cylindrical coordinates are suited to the study of the torsional Alvén waves observed in MBPs, as well as jets due to their elongated shape, and we define (r, θ, z) such that the z-axis is directed vertically upwards, perpendicular to the solar surface. Assuming a background state of equilibrium with a constant vertical magnetic field, we consider the effect of introducing a torsional Alfvén wave perturbation confined to a tube of radius R_0.

3.1. *The MHD framework*

The standard ideal MHD equations (Goedbloed & Poedts 2004) are used along with the solenoidal constraint $\nabla \cdot \mathbf{B} = 0$, but gravity is neglected, so we have

$$\rho \frac{\partial \mathbf{v}}{\partial t} + \rho(\mathbf{v} \cdot \nabla)\mathbf{v} = -\nabla p + \mathbf{j} \times \mathbf{B} \tag{1}$$

$$\frac{\partial \rho}{\partial t} + \nabla \cdot (\rho \mathbf{v}) = 0 \tag{2}$$

$$\frac{\partial \mathbf{B}}{\partial t} = \nabla \times (\mathbf{v} \times \mathbf{B}) \tag{3}$$

$$\frac{D}{Dt}\left(\frac{p}{\rho^\gamma}\right) = 0\,, \tag{4}$$

with the assumption that all quantities are independent of θ, so $\partial/\partial\theta = 0$. The quantities $\mathbf{B}, \mathbf{v}, \rho, p$ are, respectively, the magnetic field, plasma velocity, mass density, and plasma pressure, and $\mathbf{j} = \nabla \times \mathbf{B}/\mu_0$ is the current density (where μ_0 is the magnetic permeability of free space). Also, we assume that temperature is constant, and $c = \sqrt{\gamma p/\rho}$ is the sound speed, where γ is the adiabatic gas index.

3.1.1. *Perturbations*

In order to begin studying the non-linear behaviour of the Alfvén wave, we use the regular perturbation method (Hinch 1991). Let us define that each of the variables take the following functional form,

$$f(r, z, t) = f_0 + \sum_{i=1}^{\infty} \varepsilon^i f_i(r, z, t)\,, \tag{5}$$

where ε is a small expansion parameter. Here, ε is the ratio of the strength of the torsional magnetic field perturbation to that of the vertical background field within the tube. The 'zero-order' quantities are assumed to be constant and in equilibrium, so $\mathbf{v}_0 = 0$ and we define the equilibrium magnetic field $\mathbf{B}_0 = B_0\hat{z}$ to be constant and vertically aligned. The general case would require the background field and pressure to depend on r because they would be different in the interior versus the exterior region, but due to the zero-beta approximation which is assumed in this study, we find it is not necessary to make this distinction in the notation because we are able to focus only on the interior region (see Section 3.2).

In the linear approximation, we assume only a decoupled torsional Alfvén wave, which is the primary perturbation of order ε. By introducing terms of order ε^2, we now begin to consider the non-linear behaviour of the system, where we see the effect of the Lorentz force on the plasma, i.e. the manifestation of the second-order perturbation. Quantities are only defined up to order ε^2. The variables are thus perturbed in the following way,

$$\begin{aligned} v_r &= \varepsilon^2 V_{R2}\,, & v_\theta &= \varepsilon V_{\theta 1} + \varepsilon^2 V_{\theta 2}\,, & v_z &= \varepsilon^2 V_{Z2}\,, & p &= p_0 + \varepsilon^2 p_2\,, \\ B_r &= \varepsilon^2 B_{R2}\,, & B_\theta &= \varepsilon B_{\theta 1} + \varepsilon^2 B_{\theta 2}\,, & B_z &= B_0 + \varepsilon^2 B_{Z2}\,, & \rho &= \rho_0 + \varepsilon^2 \rho_2\,. \end{aligned} \tag{6}$$

The perturbed quantities are then substituted into the MHD equations. Since the features we wish to model are characterised by vertical motion of plasma according to observations, finding a solution for v_z is of particular interest.

3.1.2. *First-order approximation*

First, we neglect all terms involving square and higher powers of ε. Only the azimuthal components of the momentum and induction equations have terms of order ε,

$$\frac{\partial V_{\theta 1}}{\partial t} = \frac{B_0}{\mu_0 \rho_0}\frac{\partial B_{\theta 1}}{\partial z} \tag{7}$$

$$\frac{\partial B_{\theta 1}}{\partial t} = B_0 \frac{\partial V_{\theta 1}}{\partial z}\,. \tag{8}$$

These equations can then be combined into the wave equations for $B_{\theta 1}$, e.g.

$$\frac{\partial^2 B_{\theta 1}}{\partial t^2} = \frac{B_0^2}{\mu_0 \rho_0}\frac{\partial^2 B_{\theta 1}}{\partial z^2}\,. \tag{9}$$

The solutions to equation (9) are waves propagating in the z direction at the Alfvén speed v_A, where $v_A^2 = B_0^2/\mu_0\rho_0$. For our purposes, we consider $r, z, t \geq 0$ and use a solution for $B_{\theta 1}$ of the form

$$B_{\theta 1}(r, z, t) = f(t - z/v_A)g(r)\,. \tag{10}$$

Note we will only consider the wave travelling in the positive z-direction.

3.1.3. *Second-order approximation*

Now, we collect terms of order ε^2 in the MHD equations. The resulting system of equations shows how the torsional Alfvén waves can couple the other quantities in the system. The equations (including the solenoidal constraint) are

$$\frac{\partial B_{R2}}{\partial r} + \frac{B_{R2}}{r} + \frac{\partial B_{Z2}}{\partial z} = 0\,, \tag{11}$$

$$\rho_0\left(\frac{\partial V_{R2}}{\partial t}-\frac{V_{\theta 1}^2}{r}\right)=-\frac{\partial p_2}{\partial r}-\frac{1}{\mu_0}\left(\frac{\partial B_{\theta 1}}{\partial r}B_{\theta 1}+\frac{B_{\theta 1}^2}{r}-B_0\left(\frac{\partial B_{R2}}{\partial z}-\frac{\partial B_{Z2}}{\partial r}\right)\right), \tag{12}$$

$$\rho_0\left(\frac{\partial V_{\theta 2}}{\partial t}\right)=\frac{B_0}{\mu_0}\left(\frac{\partial B_{\theta 2}}{\partial z}\right), \tag{13}$$

$$\rho_0\left(\frac{\partial V_{Z2}}{\partial t}\right)=-\frac{\partial p_2}{\partial z}-\frac{1}{\mu_0}\left(\frac{\partial B_{\theta 1}}{\partial z}B_{\theta 1}\right), \tag{14}$$

$$\frac{\partial \rho_2}{\partial t}+\rho_0\left(\frac{\partial V_{R2}}{\partial r}+\frac{V_{R2}}{r}+\frac{\partial V_{Z2}}{\partial z}\right)=0, \tag{15}$$

$$\frac{\partial B_{R2}}{\partial t}=B_0\left(\frac{\partial V_{R2}}{\partial z}\right), \tag{16}$$

$$\frac{\partial B_{\theta 2}}{\partial t}=B_0\left(\frac{\partial V_{\theta 2}}{\partial z}\right), \tag{17}$$

$$\frac{\partial B_{Z2}}{\partial t}=-B_0\left(\frac{\partial V_{R2}}{\partial r}+\frac{V_{R2}}{r}\right), \tag{18}$$

$$\frac{\partial p_2}{\partial t}-\frac{\gamma p_0}{\rho_0}\frac{\partial \rho_2}{\partial t}=0. \tag{19}$$

From here, we wish to find out whether the model could result in the jet-like motion by obtaining a solution for V_{Z2}. We could either attempt a general solution by combining the equations and using integral transforms, or we could look for a way to simplify the mathematical framework with suitable approximations. In our initial investigations we considered the first option, but unfortunately this quickly becomes a rather complex problem because the equations are coupled. As a result we were motivated to explore the latter option, presented in section 3.2. Additionally, we are able to confirm that the approximation is compatible with the general case, shown in section 3.3.

3.2. *Zero-beta approximation*

The zero-beta approximation is applied to the region inside the tube. If the magnetic pressure dominates the plasma pressure ($\beta \ll 1$) one can neglect the pressure term in the equation of motion and so for the interior region, equation (14) becomes

$$\frac{\partial V_{Z2}}{\partial t}=-\frac{1}{2\mu_0\rho_0}\frac{\partial}{\partial z}(B_{\theta 1}^2). \tag{20}$$

This equation is then decoupled from the rest of the MHD equations, so v_r does not need to be considered. In addition, since there are no r derivatives in equation (20) and if $B_{\theta 1}$ is non-zero only within the tube, V_{Z2} is unaffected by anything in the region outside the tube in the zero-beta approximation. Note that the right-hand side of equation (20) comes from the z-component of the Lorentz force,

$$\mathbf{F_z}=(\mathbf{j}\times\mathbf{B})_z=-\varepsilon^2\frac{1}{\mu_0}\frac{\partial B_{\theta 1}}{\partial z}B_{\theta 1}, \tag{21}$$

up to ε^2 order. This force exists due to the torsional perturbation (or equivalently the shear flow $V_{\theta 1}$) and is the sole driver for the vertical acceleration of the jet in this approximation.

Once $B_{\theta 1}$ is defined (via the ε-order approximation in section 3.1.2), V_{Z2} can be found directly by integration. However, boundary conditions must also be applied. The equation can be simplified further by introducing Elsässer variables (Elsässer 1956),

$$R_\pm=v_\theta\pm\frac{v_A}{B_0}B_\theta. \tag{22}$$

Using the MHD equations we find solutions for $R_\pm$ of the form

$$R_+=R_+(t+z/v_A), \quad R_-=R_-(t-z/v_A). \tag{23}$$

We are only interested in the wave travelling in the positive z-direction, so we will have $R_+=0$ and thus

$$v_\theta=-\frac{v_A}{B_0}B_\theta. \tag{24}$$

The relationship between v_θ and B_θ means that introducing a magnetic shear perturbation has the same effect as introducing a shear flow (velocity) perturbation. Differentiating equation (24) with respect to t and then using (7), we find equation (20) becomes

$$\frac{\partial V_{Z2}}{\partial t} = \frac{1}{2\mu_0\rho_0 v_A}\frac{\partial}{\partial t}(B_{\theta 1}^2)\,. \tag{25}$$

We also apply the conditions that both V_{Z2} and $B_{\theta 1}$ are zero at $t = 0$. Integrating equation (25) directly with respect to t we can then negate any constants of integration, so we have

$$V_{Z2}(r, z, t) = \frac{B_{\theta 1}^2}{2\mu_0\rho_0 v_A}\,. \tag{26}$$

Note from equation (6) that $B_\theta^2 = \varepsilon^2 B_{\theta 1}^2 + \mathcal{O}(\varepsilon^3)$ and so, if ε is small, we find that $v_z \approx B_\theta^2/(2\mu_0\rho_0 v_A)$ to leading order.

3.3. *Relating to the general case*

Combining the second-order MHD equations from Section 3.1.3 allows us to find a fourth-order partial differential equation relating V_{Z2} and $B_{\theta 1}$,

$$\begin{aligned}&\left[\frac{\partial^4}{\partial t^4} + \left(c^2 v_A^2\frac{\partial^2}{\partial z^2} - (c^2 + v_A^2)\frac{\partial^2}{\partial t^2}\right)\left(\frac{\partial^2}{\partial z^2} + \frac{1}{r}\frac{\partial}{\partial r}\left(r\frac{\partial}{\partial r}\right)\right)\right](V_{Z2})\\ &\quad = -\frac{1}{2\mu_0\rho_0}\frac{\partial^2}{\partial t\partial z}\left\{\left[\frac{\partial^2}{\partial t^2} - v_A^2\left(\frac{1}{r}\frac{\partial}{\partial r}\left(r\frac{\partial}{\partial r}\right) + \frac{\partial^2}{\partial z^2}\right)\right](B_{\theta 1}^2) + \frac{2c^2}{r}\frac{\partial}{\partial r}\left(B_{\theta 1}^2 - \mu_0\rho_0 V_{\theta 1}^2\right)\right\}\,.\end{aligned} \tag{27}$$

The full general case requires us to also consider V_{R2} and the pressure continuity at the tube boundary, resulting in greater complexity: as well as the field-aligned force, radial forces may play a part in accelerating plasma via a 'squeezing' effect. Here, we simply aim to show how the result achieved using the zero-beta approximation fits in with the general case, without going into unnecessary detail.

Since we still require wave solutions to the first-order equations, we will use Elsässer variables as in Section 3.2. Then, from equation (24), we find that $B_{\theta 1}^2 - \mu_0\rho_0 V_{\theta 1}^2 = 0$. Thus, the final term on the right-hand side of equation (27) can be negated. Now, let $\xi = t - z/v_A$. Redefine $V_{Z2} = V_{Z2}(r, \xi)$ and $B_{\theta 1} = B_{\theta 1}(r, \xi)$ so that $\partial/\partial t = \partial/\partial\xi$ and $\partial/\partial z = -(1/v_A)\partial/\partial\xi$. Then we find that many terms in equation (27) cancel (including all terms involving the sound speed c), and so the equation can be re-written as

$$\frac{\partial^2}{\partial\xi^2}\left[\frac{\partial}{\partial r}\left(r\frac{\partial}{\partial r}\right)V_{Z2}\right] = \frac{1}{2\mu_0\rho_0 v_A}\frac{\partial^2}{\partial\xi^2}\left[\frac{\partial}{\partial r}\left(r\frac{\partial}{\partial r}\right)B_{\theta 1}^2\right]\,. \tag{28}$$

It should be noted that the result from (26) is consistent with this equation. Indeed, with suitable boundary conditions, equation (28) could be directly integrated to provide the required consistency. Thus we have further evidence to support that our zero-beta approximation method is valid for the physical configuration we model here.

3.4. *Restrictions on $B_{\theta 1}$*

The perturbation should be localised within the tube (i.e. negligible everywhere else), and it must be an Alfvén wave travelling in the positive z direction. In order to make sense physically, $B_{\theta 1}$ must be zero at $r = 0$. As previously mentioned in equation (10), $B_{\theta 1}$ can be specified as a product of some functions $f(z, t)$ and $g(r)$. We impose a boundary condition at $z = 0$ so that $f(0, t) = f_0(t)$ is non-zero only within a finite time period, $0 \le t < \tau$, where τ is the characteristic time.

The wave is introduced from the boundary at $z = 0$, before the driver is 'switched off' at the characteristic time. This results in a pulse that propagates along the flux tube, and we will have $f = f_0(t - z/v_A)$. By changing the value of τ we can scale the length of the pulse. Additionally, we will require $B_{\theta 1} = 0$ at $t = 0$, i.e. $f(z, 0) = f_0(-z/v_A)$ must be zero for all positive z.

Next, since g is so far an arbitrary function, we will define $g(r)$ so that it is only non-zero within a certain radius $0 \le r \le R_0$ corresponding to the flux tube region. Then $B_{\theta 1}$ is an Alfvén pulse which is localised in both z and r.

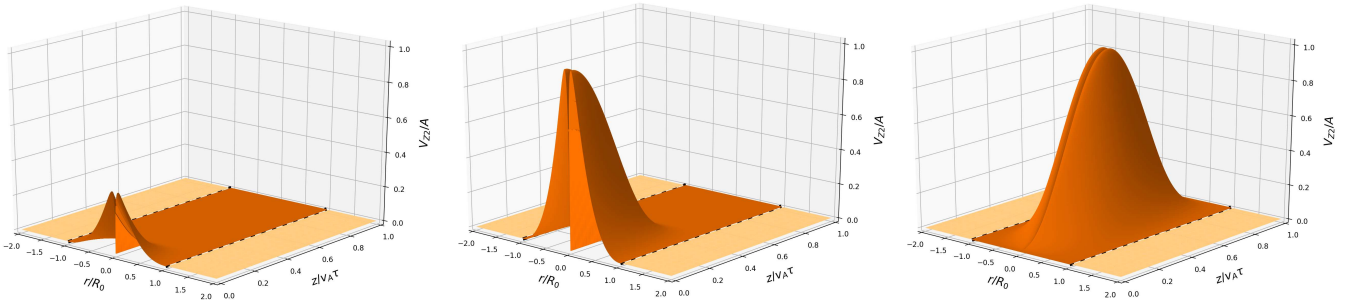

Figure 2. Above: a 2.5D representation of the given example of a V_{Z2} pulse from Section 3.5, at particular times $t = 0.2\tau$, $t = 0.5\tau$, and $t = \tau$. The pulse appears as two peaks due to the axisymmetry around the z axis of the tube, and has been rescaled so that the V_{Z2} (vertical) axis is in units of $A = B_{\max}^2/(2\mu_0\rho_0 v_A)$, while the r and z axis are in units of R_0 and $v_A\tau$ respectively. An animated version of this figure, showing the evolution of the pulse from $t = 0$ to $t = 2\tau$, is available online.

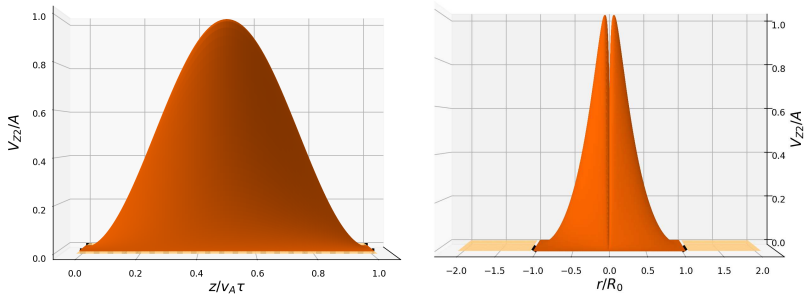

Figure 3. Rotated views of the 2.5D plot in Figure 2 at $t = \tau$, showing the z dependence (left) and the r dependence (right).

3.5. *Example solution and results*

For a more specific example using the criteria in Section 3.4, define the pulse $B_{\theta 1} = B_{\max} f(t - z/v_A)g(r)$ such that

$$f(t - z/v_A) = \sin\left(\frac{\pi(t - z/v_A)}{\tau}\right), \qquad 0 \le t - z/v_A \le \tau\,, \tag{29}$$

$$g(r) = \sin\left(\pi\,(r/R_0)^{\lambda}\right), \qquad 0 \le r \le R_0\,, \tag{30}$$

where f and g are otherwise zero and $B_{\max}$, λ are constants. We choose λ so that the pulse is localised mostly within the inner part of the flux tube; in this example $\lambda = 1/4$. The function $f(t - z/v_A)$ is non-zero only for $0 \le t - z/v_A \le \tau$ and is specified such that the characteristic time is half the period of the sine function. Recall that we also restrict the domain to $z \ge 0$ and $t \ge 0$, so $B_{\theta 1}$ is actually non-zero only when both $t \in (z/v_A,\, \tau + z/v_A)$ for any fixed z, and $z \in (z_{min},\, v_A t)$ where $z_{min} = \max\{0, v_A(t - \tau)\}$. Note that f is zero at the boundaries of these intervals and similarly g is zero at $r = 0$ and $r = R_0$, so the functions are continuous.

We solved for V_{Z2} in equation (26), in order to study the nature of the vertical motion induced by the magnetic shear and potentially explore the relationship between this type of perturbation and the mass flux observed in the chromosphere in the form of jets. The solution for V_{Z2} in the zero-beta case is simply proportional to the square of $B_{\theta 1}$,

$$V_{Z2} = \frac{B_{\max}^2}{2\mu_0\rho_0 v_A}\sin^2\left(\frac{\pi(t - z/v_A)}{\tau}\right)\sin^2\left(\pi\,(r/R_0)^{\lambda}\right), \qquad 0 \le t - z/v_A \le \tau\,, \qquad 0 \le r \le R_0\,, \tag{31}$$

and zero otherwise - see Figures 2 and 3. Hence V_{Z2} will be of a similar form to $B_{\theta 1}$, i.e. a pulse propagating in the z-direction. We suggest that a pulse in the form of this example could possibly influence plasma and contribute to the formation of a jet. Using our perturbation model we can approximate the vertical mass flux of the plasma within the locality of the pulse, $\phi_z = \rho v_z \approx \varepsilon^2\rho_0 V_{Z2}$.

Interestingly, the nature of the perturbation also suggests that there could be plasma with lower velocity near the centre of the flux tube, since we would have $\phi_z = 0$ at $r = 0$. Once the pulse is fully formed at $t = \tau$, it will maintain its shape while it propagates in the positive z direction. For $t \ge \tau$, ϕ_z will be constant on concentric toroidal surfaces,

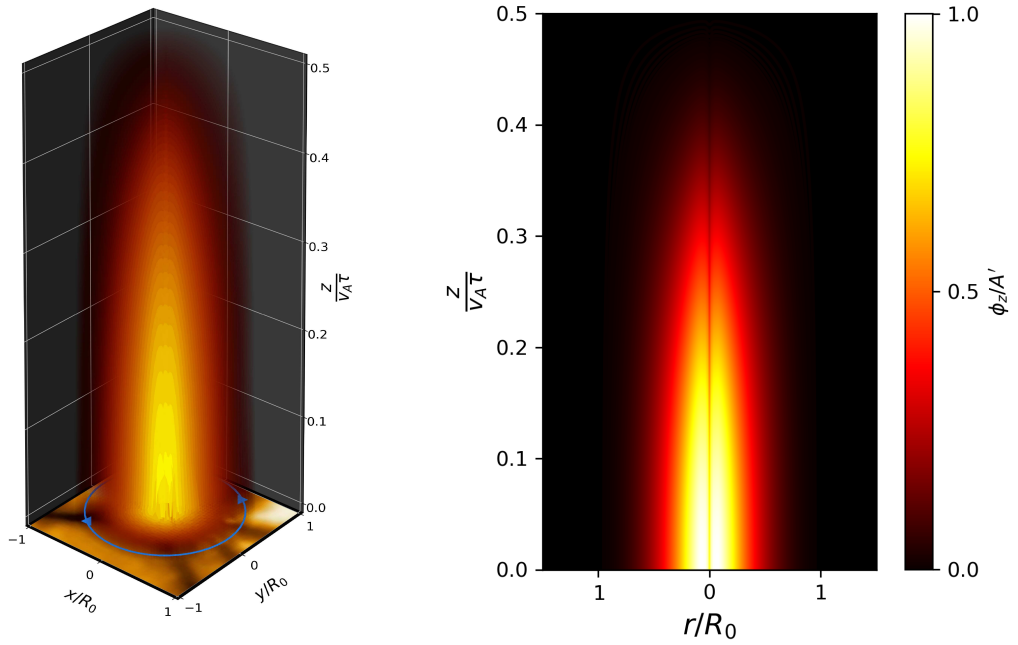

Figure 4. Left: a 3D plot of the vertical mass flux ϕ_z at time $t = \tau/2$, for the example in Section 3.5 (with scaled Cartesian axes for simplicity). At this point the pulse is 'half formed' and there is positive mass flux for $0 \leq z \leq v_A\tau/2$ within the tube. The blue arrows at the lower boundary represent the driver for the torsional magnetic field perturbation. An animated version of this figure, showing the evolution of the pulse from $t = 0$ to $t = \tau/2$, is available online. Right: a cross section of the 3D plot (on a plane of constant θ), included to illustrate the structure of the perturbation. For both plots, lighter colours denote greater magnitude of ϕ_z, but only a relative scale is given for this magnitude with $A' = B^2_{\max}/(2\mu_0 v_A)$. The magnitude approaches zero at the boundaries for which the pulse was defined in equations (29) and (30), and reaches its maximum value (dependent on the size of the perturbation of B_θ) in the interior, as shown. Although we have not specified the pulse duration τ, the pulse shown here may reach a vertical height on the order of a few Mm (depending on the Alfvén speed) at this point in time if $\tau \approx 300$s, as discussed in section 4.

which can be partially seen in Figure 4. The toroids degenerate into a cylinder, bounded by the limits for V_{Z2} stated in equation (31), as the magnitude of ϕ_z approaches zero; outside of this cylinder there is no perturbation. The maximum magnitude of ϕ_z is reached where both f and g are maximised, on the circle with radius $r = R_0/(2^{1/\lambda})$ at $z = v_A(t - \tau/2)$. Other forms of the $B_{\theta 1}$ pulse are of course possible as solutions to the first-order equations, but solutions which are suitable for the model are often similar to our example in form and behaviour.

4. DISCUSSION

The actual velocity of the plasma would depend on the magnitude of the perturbation. Despite this, the results support the idea that a torsional Alfvén wave perturbation in the magnetic field could cause plasma to be set into motion by the Lorentz force. Even a small amount of plasma lifted from the photosphere would be significant in the chromosphere, thus it is possible that this mechanism could at least contribute to the initial formation of a solar jet, although the model is not intended to accurately describe the full evolution of a physical jet. The analysis is useful as a first approximation to explore this formation mechanism.

It is clear that the vertical extent of the pulse will be approximately $v_A\tau$ simply due to the localised nature of the perturbation. We can gain more insight into this by comparing our results with observations of spicules and magnetic bright points. An Alfvén speed of 10–20 km s^{-1} is feasible inside the flux tube, based on e.g. Jess et al. (2009) and estimations from data in Hewitt et al. (2014). This is assumed to be constant in the tube, which again is a simplification. Since our model focuses mainly on the chromosphere region, it is a reasonable assumption. Then, say, at $t = 150$ s, possibly within the first half of the lifetime of a spicule and also within the range of expected lifetimes for MBPs (Keys et al. 2019), the pulse would reach a maximum vertical height of 1.5–3 Mm. Interestingly, this could also be a realistic height for a spicule in the early stages of its evolution, since spicules are observed to rise at speeds comparable to the Alfvén speed in this case (Sterling 2000). This shows that the pulse could extend to a reasonable

scale for a spicule within the time frame of the model, demonstrating a decent consistency between the model and observed properties of lower solar atmospheric jets.

In this model, we assumed ρ_0 to be constant due to the small scale of the processes we are considering compared to the height of the solar atmosphere. On a larger scale the density of the solar atmosphere decreases with height, so this model does not apply at higher elevations such as in the corona. Although the solution is a pulse which propagates to infinity, we know this would not occur in reality. For large t we expect that the solar atmosphere will deviate from the model, but the main objective was to study the effects in the photosphere and lower chromosphere since this is where the features of interest are likely to form. To improve the model, we could also take gravity and variable temperature into account. Including the ε^3-order perturbation terms would allow us to consider the back-reaction on the Alfvén wave, and we could also take into account reflection of the initial wave.

In the general case, without assuming $\beta = 0$, the model becomes more complex because the ε^2-order equations remain coupled. The equations of motion must be solved as fourth-order PDEs, and to solve for v_z we must apply the condition of continuous total pressure on both sides of the boundary of the tube in addition to boundary conditions for v_r. Due to the extra complexity it is possible that the plasma could be excited by both the Lorentz force acting vertically and by the radial 'squeezing' of the tube, causing material to be forced upwards due to the continuity of mass. The general case of this problem could be explored more thoroughly in future works.

The magnetic slab model may also be useful for investigating magnetic bright points and their role in the formation of spicules, especially the elongated bright points mentioned in Liu et al. (2018). A study using the slab model is conducted in a separate work (Oxley et al. 2020).

R.E. is grateful to Science and Technology Facilities Council (STFC, grant number ST/M000826/1) UK and the Royal Society for enabling this research. R.E. also acknowledges the support received by the CAS Presidents International Fellowship Initiative Grant No. 2019VMA052 and the warm hospitality received at USTC of CAS, Hefei, where part of his contribution was made.

REFERENCES

Athay, R. G., & Holzer, T. E. 1982, ApJ, 255, 743, doi: 10.1086/159873

Beckers, J. M. 1968, SoPh, 3, 367, doi: 10.1007/BF00171614

—. 1972, ARA&A, 10, 73, doi: 10.1146/annurev.aa.10.090172.000445

Bennett, S. M., & Erdélyi, R. 2015, ApJ, 808, 135, doi: 10.1088/0004-637X/808/2/135

Berger, T. E., Rouppe van der Voort, L., & Löfdahl, M. 2007, ApJ, 661, 1272, doi: 10.1086/517502

Berger, T. E., Schrijver, C. J., Shine, R. A., et al. 1995, ApJ, 454, 531, doi: 10.1086/176504

De Pontieu, B., Erdélyi, R., & James, S. P. 2004, Nature, 430, 536, doi: 10.1038/nature02749

De Pontieu, B., McIntosh, S., Hansteen, V. H., et al. 2007, PASJ, 59, S655, doi: 10.1093/pasj/59.sp3.S655

Dover, F. M., Sharma, R., Korsós, M. B., & Erdélyi, R. 2020, ApJ, 905, 72, doi: 10.3847/1538-4357/abc349

Dunn, R. B., & Zirker, J. B. 1973, SoPh, 33, 281, doi: 10.1007/BF00152419

Elsässer, W. M. 1956, Reviews of Modern Physics, 28, 135, doi: 10.1103/RevModPhys.28.135

Goedbloed, J. P. H., & Poedts, S. 2004, Principles of Magnetohydrodynamics (Cambridge University Press), doi: 10.1017/CBO9781139195560

González-Avilés, J. J., Guzmán, F. S., Fedun, V., et al. 2018, ApJ, 856, 176, doi: 10.3847/1538-4357/aab36f

Goodman, M. L. 2012, ApJ, 757, 188, doi: 10.1088/0004-637X/757/2/188

Haerendel, G. 1992, Nature, 360, 241, doi: 10.1038/360241a0

Hewitt, R. L., Shelyag, S., Mathioudakis, M., & Keenan, F. P. 2014, A&A, 565, A84, doi: 10.1051/0004-6361/201322882

Hinch, E. J. 1991, Perturbation methods (Cambridge University Press), doi: 10.1017/CBO9781139172189

Hollweg, J. V. 1971, J. Geophys. Res., 76, 5155, doi: 10.1029/JA076i022p05155

—. 1982, ApJ, 257, 345, doi: 10.1086/159993

Hollweg, J. V., Jackson, S., & Galloway, D. 1982, SoPh, 75, 35, doi: 10.1007/BF00153458

Innes, D. E., Inhester, B., Axford, W. I., & Wilhelm, K. 1997, Nature, 386, 811, doi: 10.1038/386811a0

James, S. P., & Erdélyi, R. 2002, A&A, 393, L11, doi: 10.1051/0004-6361:20021126

James, S. P., Erdélyi, R., & De Pontieu, B. 2003, A&A, 406, 715, doi: 10.1051/0004-6361:20030685

Jess, D. B., Mathioudakis, M., Erdélyi, R., et al. 2009, Science, 323, 1582, doi: 10.1126/science.1168680

Keys, P. H., Mathioudakis, M., Jess, D. B., et al. 2013, MNRAS, 428, 3220, doi: 10.1093/mnras/sts268

Keys, P. H., Reid, A., Mathioudakis, M., et al. 2019, MNRAS, 488, L53, doi: 10.1093/mnrasl/slz097

Kiss, T. S., Gyenge, N., & Erdélyi, R. 2017, ApJ, 835, 47, doi: 10.3847/1538-4357/aa5272

Kuridze, D., Henriques, V., Mathioudakis, M., et al. 2015, ApJ, 802, 26, doi: 10.1088/0004-637X/802/1/26

Liu, J., Carlsson, M., Nelson, C. J., & Erdélyi, R. 2019a, A&A, 632, A97, doi: 10.1051/0004-6361/201936882

Liu, J., Nelson, C. J., Snow, B., Wang, Y., & Erdélyi, R. 2019b, Nature Communications, 10, 3504, doi: 10.1038/s41467-019-11495-0

Liu, Y., Xiang, Y., Erdélyi, R., et al. 2018, ApJ, 856, 17, doi: 10.3847/1538-4357/aab150

Magyar, N., Utz, D., Erdélyi, R., & Nakariakov, V. M. 2021, ApJ, submitted

Martínez-Sykora, J., De Pontieu, B., Hansteen, V. H., et al. 2017, Science, 356, 1269, doi: 10.1126/science.aah5412

Mathioudakis, M., Jess, D. B., & Erdélyi, R. 2013, SSRv, 175, 1, doi: 10.1007/s11214-012-9944-7

Matsumoto, T., & Shibata, K. 2010, ApJ, 710, 1857, doi: 10.1088/0004-637X/710/2/1857

Oxley, W., Scalisi, J., Ruderman, M. S., & Erdélyi, R. 2020, ApJ, 905, 168, doi: 10.3847/1538-4357/abcafe

Raouafi, N. E., Patsourakos, S., Pariat, E., et al. 2016, SSRv, 201, 1, doi: 10.1007/s11214-016-0260-5

Roberts, B. 1979, SoPh, 61, 23, doi: 10.1007/BF00155443

Rouppe van der Voort, L., Leenaarts, J., de Pontieu, B., Carlsson, M., & Vissers, G. 2009, ApJ, 705, 272, doi: 10.1088/0004-637X/705/1/272

Ryutova, M. 2015, Physics of Magnetic Flux Tubes, Vol. 417 (Springer-Verlag Berlin Heidelberg), doi: 10.1007/978-3-662-45243-1

Samanta, T., Tian, H., Yurchyshyn, V., et al. 2019, Science, 366, 890, doi: 10.1126/science.aaw2796

Sánchez Almeida, J., Bonet, J. A., Viticchié, B., & Del Moro, D. 2010, ApJL, 715, L26, doi: 10.1088/2041-8205/715/1/L26

Secchi, A. 1877, L'astronomia in Roma nel pontificato DI Pio IX. (Tipografia della Pace, Roma)

Shibata, K., & Uchida, Y. 1985, PASJ, 37, 31

—. 1986, SoPh, 103, 299, doi: 10.1007/BF00147831

Smith, M. D. 2012, Astrophysical Jets and Beams (Cambridge University Press), doi: 10.1017/CBO9780511994562

Sterling, A. C. 2000, SoPh, 196, 79, doi: 10.1023/A:1005213923962

Sterling, A. C., Moore, R. L., & DeForest, C. E. 2010, ApJL, 714, L1, doi: 10.1088/2041-8205/714/1/L1

Suematsu, Y. 1980, in Japan-France Seminar on Solar Physics, ed. F. Moriyama & J. C. Henoux (Tokyo Astronomical Observatory, The University of Tokyo), 66

Tsiropoula, G., Tziotziou, K., Kontogiannis, I., et al. 2012, SSRv, 169, 181, doi: 10.1007/s11214-012-9920-2

Verwichte, E., Nakariakov, V. M., & Longbottom, A. W. 1999, Journal of Plasma Physics, 62, 219, doi: 10.1017/S0022377899007771

Withbroe, G. L., Jaffe, D. T., Foukal, P. V., et al. 1976, ApJ, 203, 528, doi: 10.1086/154108

Zaqarashvili, T. V., & Erdélyi, R. 2009, SSRv, 149, 355, doi: 10.1007/s11214-009-9549-y